HADES EXPERIMENTS: INVESTIGATION OF HADRON IN-MEDIUM PROPERTIES*

Piotr Salabura†, Witold Przygoda‡

The Marian Smoluchowski Institute of Physics, Jagiellonian University
Reymonta 4, 30-052 Kraków, Poland

(Received January 28, 2014)

Hadron modifications in nuclear matter are discussed in connection to chiral symmetry restoration and/or hadronic many body effects. Experiments with photon, proton and heavy ion beams are used to probe properties of hadrons embedded in nuclear matter at different temperatures and densities. Most of the information was gathered for the light vector mesons ρ, ω and ϕ. HADES is a second generation experiment operating at GSI (Darmstadt) with the main aim to study in-medium modifications by means of dielectron production at the SIS18/Bevelac energy range. Large acceptance and excellent particle identification capabilities allow also for measurements of strangeness production. These abilities combined with the variety of beams provided by the SIS18 lead to a characterization of properties of the dense baryonic matter properties created in heavy ion collisions at these energies. A review of recent experimental results obtained by HADES is presented, with the main emphasis on hadron properties in nuclear matter.

DOI:10.5506/APhysPolB.45.799
PACS numbers: 27.75.Dw, 13.30.–a, 13.40.Hq, 13.75.–n

1. Introduction

Sizeable spectral modifications have been predicted by various theoretical models for hadrons embedded in cold or hot and dense nuclear matter. In this respect, most attention has been focused on properties of the light vector mesons (ρ, ω and ϕ) as probes of chiral symmetry restoration (for reviews, see [1, 2]). Early work based on QCD sum rules suggested a direct link between changes of the meson masses and QCD vacuum properties, characterized by a reduction of the expectation value of the two-quark condensate [3, 4]. More

* Presented at the II International Symposium on Mesic Nuclei, Kraków, Poland, September 22–25, 2013.

† piotr.salabura@uj.edu.pl
‡ witold.przygoda@uj.edu.pl

recent work shows that, however such a link indeed exists, it is much more sophisticated than originally thought and offers a rather limited predictive power [1].

On the experimental side, a lot of activities have been carried out over the last years investigating the light vector meson production off nuclei with proton and photon beams and in heavy ion reactions. Two experimental approaches have been used to identify in-medium modifications of the vector mesons: *(i)* directly, via the reconstruction of their invariant mass distribution from the detected decay products and *(ii)* by quantifying the meson absorption in nuclei from the production yields and by connecting it to the in-medium width $\Gamma^*_{\rm tot}$ by model calculations (this method is used for $p(\gamma)+A$ collisions). The best suited final state are dileptons, which does not suffer strong final state interactions (FSI) with the nuclear matter, but one has to cope with the small branching ratios ($\sim 10^{-5}$). The densities and temperatures reached in heavy ion collisions are, of course, higher, and larger effects can be expected but one has to model properly the time evolution of the collision system to calculate dilepton radiation. Moreover, in order to access the true in-medium radiation, one has to subtract the contribution of mesons decaying in the late state of the heavy ion collision, that is after the so called "freeze-out" where all interactions between the produced particles have ceased.

Results from $p(\gamma)-A$ experiments are somehow controversial: while the E325 experiment at KEK claims [5] the observation of a mass drop of the ρ meson in the e^+e^- invariant mass spectrum according to the Brown–Rho scaling [4], investigations at JLAB (CLAS) [6] do not corroborate such a conclusion showing only slight broadening of the ρ. Transparency measurements for the ω at ELSA/MAMI (CBELSA-TAPS) [7] and JLAB [8], and ϕ at COSY (ANKE) [9], LEPS at Spring8 [10] indicate large absorption of both mesons.

In heavy-ion collisions, the search for vector meson spectral modifications via dilepton spectroscopy was pioneered by the CERES [11] and HELIOS [12] collaborations at the CERN-SPS and the DLS experiment [13] at Bevalac. A low-mass pair excess, below the ρ/ω pole, above the yield expected from free hadron decays after the freeze-out was reported and widely discussed in many theoretical papers (for a review, see [2]). Although the limited statistics of these experiments did not allow to derive firm conclusions, results obtained at SPS indicate that the excess is related to pions annihilating into the ρ meson, hence it is directly linked to the ρ in-medium spectral function. The breakthrough in this field was achieved with the high-statistics NA60 data set which allowed, for the first time, to extract in-medium spectral function of the ρ meson [14]. Comparisons to various theoretical calculations show that the spectral function is mainly affected by two in-medium

effects: *(i)* modification of the pion loop in the ρ meson self-energy and *(ii)* direct rho-meson couplings to low-mass baryon resonance-hole excitations [15]. Furthermore, it appears that the second mechanism plays the essential role in the observed melting of the ρ meson in hot and dense nuclear matter. On the other hand, the naive mass dropping scenario was found to be not supported by the data. At the top RHIC energies, the situation is less clear: first results from the most central Au + Au collisions at $\sqrt{s} = 200$ GeV obtained by PHENIX indicated even larger excess than at SPS [16]. However, new measurements performed by STAR (see contributions to this conference) do not corroborate this observation.

On the opposite side of the energy scale, at 1–2 AGeV, results of the DLS experiment could not find a satisfactory explanation for a long time. Dielectron spectra measured even in light C + C collisions were not described by any model calculation showing a large excess in the mass $0.15 < M_{e^+e^-} < 0.6$ GeV/c^2 range. However, nuclear matter probed in this energy range is dominated by baryons (nucleons and up to 30% low mass-baryonic resonances) and it has a different composition from the meson (mainly pion) dominated once probed at SPS. Therefore, it was not clear if the excess is due to some particular features of baryonic sources not properly modelled in the calculations or true in-medium effects.

A clarification of this dilemma was one of the main reasons to build the HADES experiment at GSI [17]. It is a second generation versatile detector with excellent particle identification capabilities and large acceptance. HADES (High Acceptance DiElectron Spectrometer) has, for the first time in this energy regime, the capability to simultaneously measure various rare probes like dielectrons, single (kaons, hyperons) and double strange hadrons ($\Xi^-(1321)$) and ϕ mesons. The ability to study strangeness production is particularly interesting from the point of view of still unsettled questions of kaon in-medium properties (for a review, see [18]). Experiments performed at GSI by means of KAOS and FOPI detectors provided many interesting data. However, further precise measurements of kaon flow, low transverse momentum distributions of kaons and ϕ production are necessary to fully characterize kaon production in heavy ion collisions. Furthermore, double strange hyperons have never been measured before at SIS18 energies and likewise first data on ϕ meson production have been only recently provided by HADES and FOPI detectors.

2. Experimental programme of HADES

The HADES programme can be divided into three strongly interconnecting parts. Experiments studying dielectron, pion and baryon resonance production in proton–proton (at 1.25, 2.2 and 3.5 GeV) and $d+p$ (at 1.25 GeV)

reactions provided important constraints on contributions of various e^+e^- sources and allowed to establish model independent reference spectra for studies of proton–nucleus and nucleus–nucleus collisions. $p+p$ collisions at 3.5 GeV provided also valuable new data on hyperon $\Sigma(1385)$ and $\Lambda(1405)$ production. The vector mesons and the neutral kaon productions were investigated in $p+\mathrm{Nb}$ collisions at 3.5 GeV to search for meson modifications in cold nuclear matter. Small $\mathrm{C}+\mathrm{C}$, medium $\mathrm{Ar}+\mathrm{KCl}$ and large size $\mathrm{Au}+\mathrm{Au}$ collision systems were explored in the 1–2 AGeV energy range to study dielectron and strangeness production (ϕ, $K^{-,+,0}$, Λ, $\Xi^-(1321)$).

Using the variety of proton, deuteron and ion beams, HADES can study elementary and heavy ion reactions creating dense (up to $3\rho_0$) and hot (with temperatures up to $T = 80$ MeV) nuclear matter with relatively long life time (~ 10 fm/c). With its future scientific programme at SIS100 at FAIR it will also cover the 8–10 AGeV energy range, where there is no dielectron data up to now. Below, we present highlights of the results obtained so far, with the emphasis on hadron in-medium properties.

3. Results from N–N collisions

The special character of e^+e^- production in N–N collisions in the 1–2 GeV beam energy range is given by a strong contribution of baryonic sources: Dalitz decays of nucleon resonances $R \to Ne^+e^-$ (mainly $\Delta(1232)$) and N–N bremsstrahlung, and a strongly rising excitation functions of the η meson production [19]. The baryonic sources completely determine the e^+e^- invariant mass distribution above the π^0 mass at beam energies below the η-meson production threshold ($E^{\mathrm{thr}}_{\mathrm{beam}} = 1.25$ GeV) [20]. The latter contributes via $\eta \to e^+e^-\gamma$ decay at the same level as the baryonic sources already around 1.6 GeV. The vector meson production is small because of the high production threshold ($E^{\mathrm{thr}}_{\mathrm{beam}} = 1.88$ GeV for ω) and adds an important contribution to the invariant mass spectrum at $M_{e^+e^-} > 0.6$ GeV/c^2. While the exclusive ω and η production in $p+p$ reactions close to the production threshold is very well known, the data on ρ are scarce. Furthermore, in contrast to the ω and ϕ production mechanisms, which essentially do not show resonance contributions, a strong coupling of the ρ meson to the low-mass baryonic resonances ($D_{13}(1520)$, $P_{13}(1720)$, $S_{31}(1620)$) has been predicted by many models (see, for example, [21, 22]). Since the ρ meson is a broad resonance, these couplings can lead to the spectral function very different from a simple Breit–Wigner distribution even in elementary reactions. One should underline that a detailed understanding of these couplings is a prerequisite for any conclusions on in-medium modifications in nuclear matter. This statement holds also for the situation at higher beam energies where, as already discussed above, baryonic effects are of major importance

for the interpretation of NA60 and CERES data. One should also stress that decays processes like $R \to Ne^+e^-$ (Dalitz) and $R \to \rho(\to e^+e^-)N$ are strongly linked and should not be, in general, treated as two separate decay channels. A natural connection should be provided by a structure of the electromagnetic transition form factors in the time-like region, *i.e.* its dependence on the virtual photon (or e^+e^- invariant) mass. Calculations performed within the extended Vector Meson Dominance (VMD) model [23] and the two component models [24, 25] indeed show the importance of the vector mesons in such transitions. However, new precise data from proton and, in particular, pion induced reactions on such decays are needed to provide more constraints for calculations. We come to this issue in the discussion of the HADES data obtained at higher beam energy of 3.5 GeV (next chapter).

Another feature of dielectron production in $N + N$ reactions is a very strong isospin dependence. This feature was already demonstrated by the DLS experiment measuring excitation functions of the pair production in $p + p$ and $d + p$ collisions in the beam energy range E_{beam}1–4.88 GeV [26]. Though the statistics gathered in these experiments is limited and the systematic errors related to normalization are large, one can clearly see that there is a strong increase of the non-trivial pair yield (in the $M_{e^+e^-} > M_{\pi^0}$ range) in $d + p$ reactions over the one measured in $p + p$ below 2 GeV, with maximum around $E_{\mathrm{beam}} = 1.25$ GeV. New data obtained by HADES stimulated significant progress in understanding of this phenomenon. Fig. 1 shows the e^+e^- invariant mass distributions obtained in $p + p$ and, for the first time, in quasi-free $n + p$ reactions, the latter one selected by tagging the proton spectator from $d + p$ collisions, at $E_{\mathrm{beam}} = 1.25$ GeV. While the $p + p$ data can be described rather well by the incoherent superposition of the π^0 and $\Delta(1232)$ Dalitz decays, the $p + n$ data show a large excess over these two contributions at $M_{e^+e^-} > M_{\pi^0}$. The situation is not changing by adding a small η contribution in the $p + n$ case, appearing because of the neutron momentum distribution inside deuteron. The latter one is very well constrained by the known η meson production cross section and nucleon momentum distribution inside the deuteron (for details, see [20]). The shaded area shows the uncertainty related to the electromagnetic transition form-factor of the $\Delta(1232) \to Ne^+e^-$ decay calculated here within the Iachello–Wan model [25]. The solid curve shows predictions of [27] based on One Boson Exchange model of the bremsstrahlung process taking into account the coherent sum of resonant ($\Delta(1232)$) and non-resonant (so-called "quasi-elastic" bremsstrahlung) contributions [27]. In Fig. 2, we show results of the OBE calculations [28], based on similar diagrams, compared to HADES data which provide a slightly better description of both collision systems. In particular, the very different shape of the $p + n$ data is better

accounted for, due to the incorporation of the electromagnetic form factor of the charged pion. This contribution is possible since, unlike in the $p+p$ reaction, a charged pion can be exchanged.

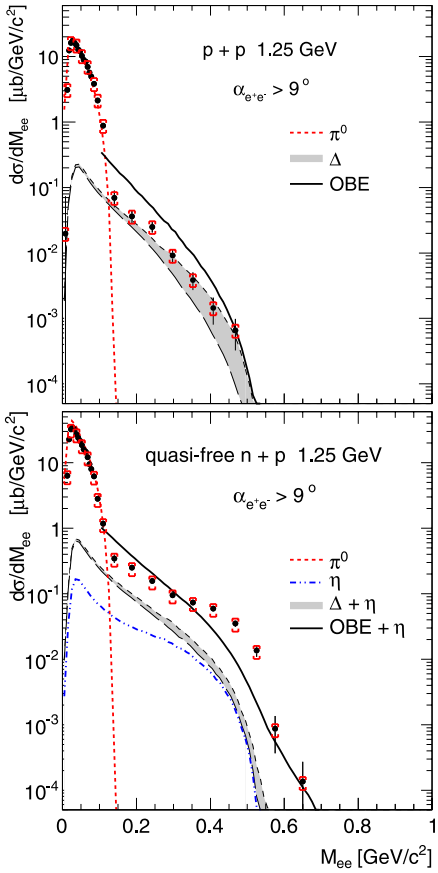

Fig. 1. Electron pair differential cross sections as a function of invariant mass (full circles) measured in $p+p$ reactions (upper panel) and in quasi-free $n+p$ reactions (lower panel) at 1.25 GeV. Systematic errors (constant in the whole mass range) are indicated by (dark grey/red) horizontal bars, statistical errors by vertical bars. Expected contributions from π^0, $\Delta(1232)$ and η Dalitz decays obtained by PLUTO event generator are shown separately [20]. Solid curves show predictions from the One Boson Exchange Model [27].

Another interesting possibility to explain the $p+n$ data has been recently suggested by Clement and Bashkanov [29] in connection to two-pion production channels. In their model, explaining very well two-pion production in $p+p$ and $p+n$ reactions, the dielectron enhancement observed in

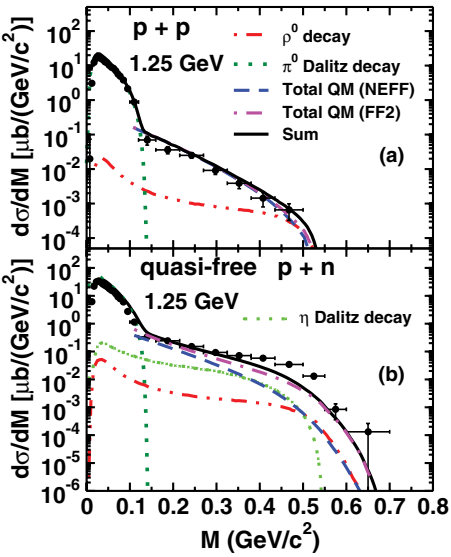

Fig. 2. Experimental data (the same as in Fig. 1) compared to the One Boson model [28]. Results without (NEFF) and with (FF2) incorporation of the electromagnetic form factor of charged pions are shown separately. Solid curves show sum of these contributions with the subthreshold ρ production.

$p + n$ originates from double delta excitation followed by the subsequent decay into dielectron pair in the isospin $I = 1$ channel, strongly coupled to off-shell ρ meson.

Although, the theoretical description of the $p + n$ data is not yet finally settled, the data allow to construct the experimentally derived $N + N$ reference spectrum, which we use for heavy ion reactions to account for the contribution of the baryonic sources.

4. Results from p–A collisions

$p + p$ and $p +$ Nb collisions at a beam energy of 3.5 GeV have been studied by HADES with the main goal to search for in-medium modification of vector mesons in cold nuclear matter. The large acceptance of the detector and the low energy of the beam allow for detection of e^+e^- pairs down to momenta as low as $p_{e^+e^-} < 1.0$ GeV/c, not accessible in the CLAS and E325 experiments. Differential inclusive e^+e^- production cross sections as a function of the e^+e^- invariant mass (shown in Fig. 3), the momentum and the rapidity have been measured for both reactions [32]. The direct comparison of the measured distributions to the yields expected from the known hadronic sources (from the PYTHIA calculation) is shown for $p+p$ collisions

in Fig. 3 [30]. It reveals an unexplained strength below the vector meson pole which becomes even more pronounced in proton–nucleus collisions. As already discussed in the previous sections, one can expect such additional strength by a strong coupling of the ρ meson to low-mass baryonic resonances, which are not included in PYTHIA. On the other hand, there are no higher mass resonances, besides $\Delta(1232)$ included in the calculations. In order to shed more light on this problem, the exclusive ppe^+e^- channel was investigated. Such a channel selects, from many other possible dielectron sources, only those which are related to the two-body vector meson decays and the resonance conversions $R \to pe^+e^-$. The other dielectron sources

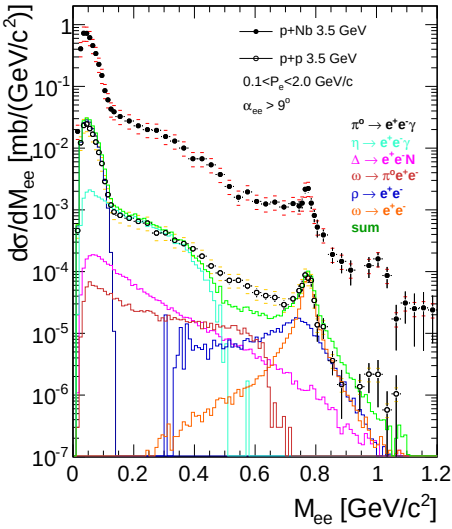

Fig. 3. Comparison of dielectron cross sections as a function of the invariant mass measured in $p+p$ and $p+\mathrm{Nb}$ collisions at the kinetic beam energy of 3.5 GeV. For $p+p$ data, the PYTHIA dilepton cocktail composed of various e^+e^- sources, defined in the legend, is displayed in addition [32].

dominating in the inclusive e^+e^- production, in particular the Dalitz decays of $\eta(\pi^0) \to e^+e^-\gamma$ and $\omega \to \pi^0 e^+e^-$, can be effectively suppressed via kinematical constraints. Figure 4 displays the e^+e^- invariant mass distribution for the ppe^+e^- events. It is compared to the simulation including dielectron sources originating from the baryon resonance $R \to pe^+e^-$, R is $\Delta(1232)$ (black/red solid line) and higher mass Δ^+, N^* (grey/green solid line), and the two-body meson $\rho, \omega \to e^+e^-$ decays. The respective production cross sections for the baryonic resonances were extracted from the one pion production data taken in the same experiment (the hatched area indicated errors related to the extracted cross sections). The branching ratios

for the resonance conversion were calculated assuming point-like $R\gamma^*$ couplings fixed by the known $R \to \gamma N$ partial decay widths (for more details, see [31]). The calculation underestimates the data, hence corroborates the hypothesis of a strong off-shell resonance-ρ coupling, enhancing dielectron emission below the vector meson pole. Indeed, model calculations based on a resonance model assuming that dilepton decays of resonances proceed via a two step process $R \to \rho N \to N e^+e^-$ explain the data very well [21, 31]. The strongest contributions, besides $\Delta(1232)$ come from $D_{13}(1520)$, S_{31} (1620), $P_{13}(1720)$ and $F_{35}(1905)$, however, one should mention that branching ratios into ρN are a subject of large uncertainties.

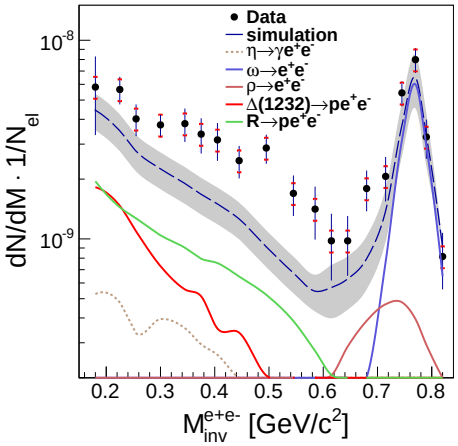

Fig. 4. e^+e^- invariant mass distributions compared to the simulation result assuming a point-like $RN\gamma^*$ coupling ("QED-model"). The hatched area indicates the model errors (for more details, see the text) [31].

Coming back to the $p + \mathrm{Nb}$ data, we show in Fig. 3 comparison of the e^+e^- invariant mass distribution to the one measured in $p + p$ reactions for low dielectron momenta $p_{e^+e^-} < 0.8$ GeV/c. Here, the $p + p$ cross sections have been scaled up by a ratio of the total cross sections for both reactions and the averaged numbers of participants calculated with a Glauber model: $\sigma_{p\mathrm{Nb}}/\sigma_{pp} \times \langle A^{p\mathrm{Nb}}_{\mathrm{part}}\rangle / \langle A^{pp}_{\mathrm{part}}\rangle$. With such a scaling, π^0 production measured in $N + N$ describe our C + C data (see the next section) and also, (see Fig. 3) pion Dalitz yield in $p + \mathrm{Nb}$. On the other hand, a strong increase of the e^+e^- yield below the vector meson pole above the $p + p$ reference is visible.

In order to better quantify this excess we subtract, first, the ω peak in both data samples and further subtract the scaled $p + p$ dielectron yield from the $p + \mathrm{Nb}$ yield. The difference, shown in Fig. 5 (right panel), represents the additional e^+e^- radiation excess due to the medium. For the scaled spectra, the resulting excess for $p_{e^+e^-} < 0.8$ GeV/c corresponds to

a factor 1.5 ± 0.3 more than the $p+p$ data in the invariant mass region between 0.3 and 0.7 GeV/c^2 and shows an exponential decrease with an additional enhancement directly below the vector meson pole mass, *i.e.* between 0.6–0.7 GeV/c^2. Note that this enhancement is exactly at the position where a discrepancy is observed when comparing the $p+p$ data with the PYTHIA calculation (Fig. 3). This might be interpreted as a fingerprint of the secondary processes, *i.e.* $p+p \to \pi X$, $\pi N \to R \to Ne^+e^-$ contributing also to this mass region because of the aforementioned strong resonance-ρ couplings. On the other hand, most of model calculations based on hadronic many-body interactions predict that such couplings strongly modify the in-medium ρ meson spectral function. Therefore, final conclusions about in-medium modifications of the ρ meson in cold nuclear matter can be derived only if a consistent treatment of the spectral shape of the meson in the medium together with a correct handling of the additional yield from secondary reactions is achieved.

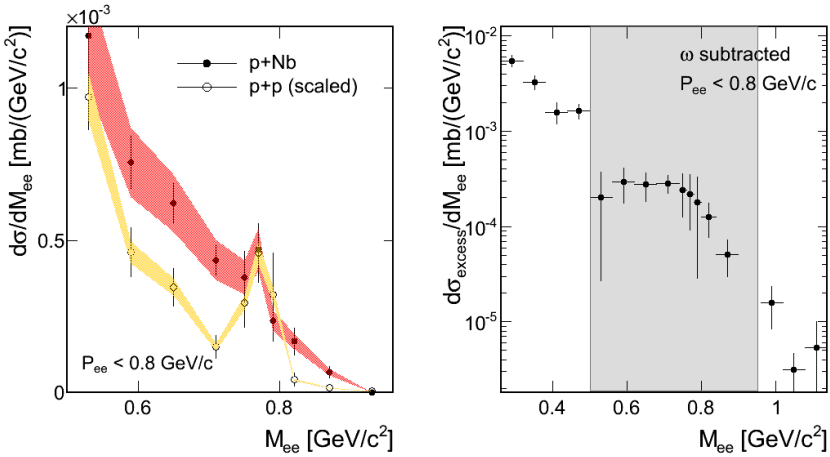

Fig. 5. Left: the same as in Fig. 3 but zoomed into the vector meson region. The shaded bands represent the systematic uncertainties due to the normalization. Right: excess yield in the $p+$Nb data after subtraction of the scaled $p+p$ reference data (the ω contribution has been subtracted in both data samples). The grey region corresponds to the invariant mass range plotted in the left picture [32].

As the ω meson is concerned, we observe that for slow pairs the yield at the ω pole is not reduced, however, the underlying smooth distribution is enhanced. Thus, the yield in the peak is almost zero within the errors. This indicates a strong ω absorption in contrast to the pairs from the underlying continuum. Assuming that the ω cross section scales with the mass number as $\sigma_{p\mathrm{Nb}} = \sigma_{pp} \times A^{\alpha}$, we obtain $\alpha = 0.38 \pm 0.29$ for slow pairs and $\alpha = 0.67 \pm 0.11$ for $p_{e^+e^-} > 0.8$ GeV/c. Furthermore, the analysis of

the ω width shows, within the error bars, no significant broadening. Both observations are in line with the results of the CBELSA-TAPS experiment [33], although one should note that in contrast to the $p+A$ reactions for the photon induced reactions no initial state effects and consequently a stronger scaling could be expected.

5. Results from A–A collisions

In the 1–2 AGeV energy range, particle production in heavy-ion collisions is dominated by pion production which originates mainly from the $\Delta(1232)$ resonance. Multiplicities of heavier mesons, mainly η, are already very low (of the order of 1–2%). Production multiplicities for π^0 and η mesons are known from their decay into real photons from former TAPS measurements at GSI [34]. The dielectron invariant-mass distributions measured with HADES in the light C + C (at 1.0 AGeV) [35] and the medium-heavy Ar + KCl (at 1.756 AGeV) [36] systems are shown in Fig. 6.

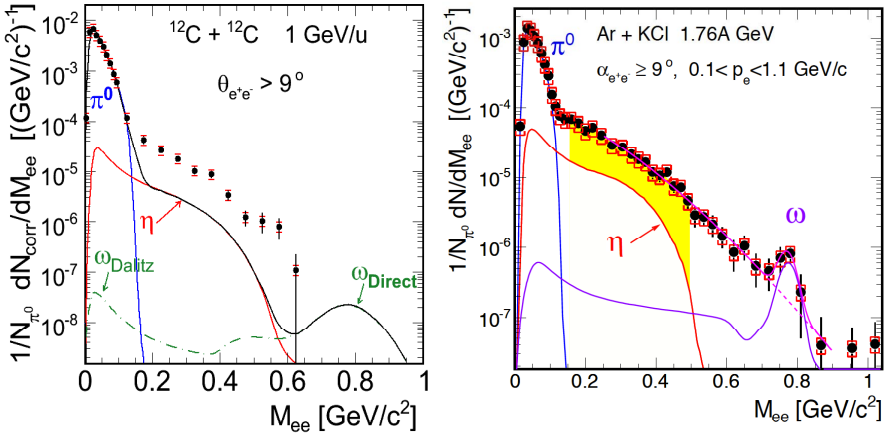

Fig. 6. Left: e^+e^- production rates normalized to the π^0 yield as a function of the invariant-mass distribution measured in C + C collisions at 1 AGeV compared to thermal dielectron cocktail of mesonic sources (π^0, η, ω) after freeze-out [35]. Right: similar distributions but obtained for Ar + KCl collisions at 1.756 AGeV [36]. Shaded area shows invariant mass region where the pair excess from in-medium radiation has been identified (for details, see the text). Different widths of the ω peak in simulated cocktails accounts for different mass resolution in both experiments.

The spectra are normalized to the mean of the charged pion (π^+, π^-) yields, measured independently by HADES, and extrapolated to the full solid angle. At this energy and for these collision systems, it is a good measure of neutral pion multiplicity. The differential distributions obtained in

such a way are compared to the expected mesonic e^+e^- cocktail from the π^0, η Dalitz and ω decays according to the measured (for π^0 and η) and extrapolated (from the m_{T} scaling for ω) multiplicities. One should underline that the ω peak visible in the invariant mass distribution in Ar + KCl collisions allows for the first measurement of meson production at such a low energy (below its free N–N threshold). As one can see, the e^+e^- cocktail composed from the meson decays does not explain the measured yields for both collision systems and leaves room for a contribution expected from the baryonic sources discussed above: resonance Dalitz decays (mainly $\Delta(1232)$) and nucleon–nucleon bremsstrahlung. This conclusion is also supported by our analysis of the shape of excitation function of the missing contribution that appears to be very similar to the one measured for pions, governed by $\Delta(1232)$ creation, but very different from the one established for the η meson [36].

In order to search for a true in-medium radiation off the dense nuclear phase of collisions, we compare e^+e^- production rates found in nucleus–nucleus reactions with a proper superposition of the production rates measured in elementary collisions. For this purpose, we plot in Fig. 7 the ratio of the pair multiplicities measured in nucleus–nucleus collisions, shown in Fig. 6 (and also for C + C at 2 AGeV), to the averaged $1/2(M_{pp}^{e^+e^-} + M_{pn}^{e^+e^-})/M_{\pi^0}$ obtained from the e^+e^- cross sections shown in Fig. 1 and the known π^0 cross section for the elementary reactions. Furthermore, before the ratios are computed, we subtract for all distributions the respective η Dalitz contribu-

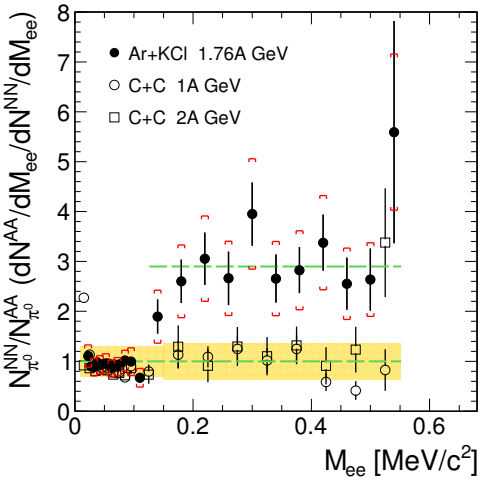

Fig. 7. Ratio of e^+e^- invariant mass distributions measured in Ar + KCl and C + C with subtracted η meson contribution to the $N + N$ reference spectrum, obtained as described in the text. Total errors, statistical and systematic are added quadratically and indicated by the shaded band [36].

tions. The latter is motivated by a very different excitation function of the η meson production in nucleus-nucleus and nucleon–nucleon reactions and hence allows for comparison of collision systems measured at different beam energies. Normalization to the M_{π^0} takes into account the beam energy dependence of baryonic sources discussed above and also the dependence of particle production on system-size via scaling with an average number of participants A_{part}, which holds at SIS18 energy range (for more details, see [36]). As one can see, all distributions agree in the π^0 mass range confirming our normalization procedure. Furthermore, the ratio is consistent, within statistical and systematic errors, with the one for C + C collisions at 1 and 2 *A*GeV. It means that indeed, pair production in the mass range $M_{e^+e^-} < 0.6$ GeV/c^2 in C + C collisions can be described as a sum of contributions stemming from *(i)* baryonic sources, extracted from the $N + N$ collisions, which yield scale as pion production and *(ii)* the η, π^0 mesons accounting for the radiation after freeze-out. This observation explains the long standing "DLS puzzle" of the unexplained yield measured in C + C collisions by not correctly accounted baryonic contributions. In this context, we emphasize that the DLS and HADES data agree within errors bars as shown by the dedicated analysis [35].

However, a significant excess (2.5–3) with respect to the $N + N$ reference is visible for the Ar + KCl system above the π^0 mass, indicating an additional contribution from the dense phase of the heavy ion collision. This means that going to the larger collision system Ar + KCl (A_{part} for Ar + KCl $\simeq 40$ should be compared to $A_{\mathrm{part}} \simeq 8$ for C + C for our trigger conditions) a stronger than linear scaling of the pair production with A_{part} is observed. This observation can be interpreted as a signature of the onset of a contribution of multi-body and multi-step processes in the hot and dense phase created in collisions of nuclei of sufficiently large size. In this context, the propagation of short-lived baryonic resonances seems to play a major role. The penetrating nature of the dilepton probe allows to observe an effect of "shining" of the baryonic matter integrated over the whole collision time. A further important test of this scenario will be provided by data recently obtained from Au + Au collisions at 1.25 *A*GeV.

Interesting new results on the vector meson production in heavy-ion collisions at SIS18 have also been obtained from analysis of Ar + KCl data. Besides the ω signal discussed above, a surprisingly strong ϕ meson production has been found from the analysis of the K^+K^- final state (see Fig. 8) [37]. The acceptance corrected ϕ/K^- ratio is found to be 0.37 ± 0.13 which translates into a fraction of $18 \pm 7\%$ of negative kaons coming from ϕ decay. Furthermore, assuming that non-resonant K^+K^- production is of the same size, as it is known from $N + N$ reactions, an even larger contribution of reactions other than strangeness exchange (π^- hyperon $\rightarrow K^-N$),

assumed before to be the dominant process in K^- production, should be expected. This, for example, can indicate that the ϕ meson is produced in a multi-step processes involving short-lived resonances. Such scenario is corroborated by the BUU transport calculations [38] which reproduce the yields and spectral distributions of K^+K^- and ϕ mesons.

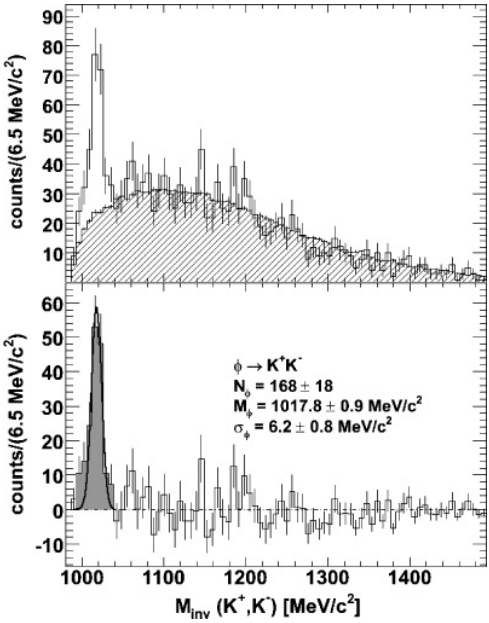

Fig. 8. Invariant mass distribution of K^+K^- pairs (top). The combinatorial background (shaded area) is obtained by the mixed-event technique. The background-subtracted distribution (bottom) shows a ϕ-meson signal (grey area with a Gaussian fit) [37].

Figure 9 shows the ratio of the ϕ to ω multiplicities measured in Ar + KCl collisions at 1.756 AGeV, together with predictions of the statistical model THERMUS and results from elementary reactions [36, 37]. The data points are plotted as a function of the excess energy above the production threshold for the exclusive ϕ production in $p + p$ and $\pi + N$ reactions, respectively. One can see from this comparison that in the heavy-ion reaction $R_{\phi/\omega}$ is more than one order of magnitude larger than in $N + N$ collisions and also at least a factor 3–5 larger than in pion-induced processes. On the other hand, the ratio is consistent with the thermal model assuming full thermalization and no suppression due to OZI rules. The ratio could, of course, also be influenced by different absorption processes of both mesons in nuclear matter. Indeed, the results from cold matter experiments, mentioned in the introduction, indicate larger absorption of the ω meson as compared

to the ϕ what could enhance the in-medium $R_{\phi/\omega}$. The effect of ω absorption and the absence of such effect on the ϕ was also observed by NA60 in In + In collisions at 158 AGeV [39, 40].

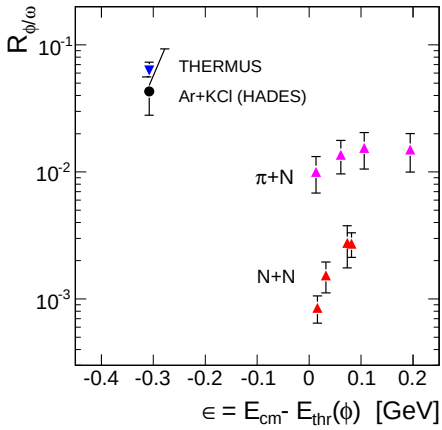

Fig. 9. Comparison of the measured $R_{\phi/\omega}$ ratio (HADES) and statistical model value (THERMUS fit) as well as a compilation of data from the $p + p$ and $\pi + N$ reactions (see the text). The ratio is plotted as a function of the excess energy above the threshold for the exclusive production in $p + p$ and $\pi + N$ reactions [36].

In-medium effects on kaons have been studied by means of K^0_S meson transverse momentum distributions in Ar + KCl collisions at 1.76 AGeV taking advantage of the good acceptance of HADES at low transverse momentum for the $K^0_S \to \pi^+\pi^-$ reconstruction [41]. We compared p_t distributions for different rapidity bins with the corresponding results by the IQMD trans-

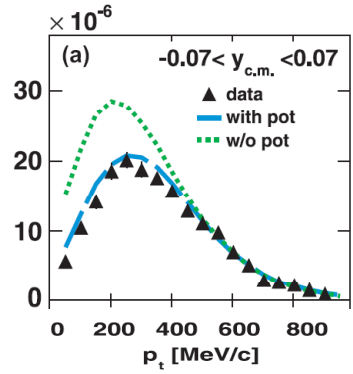

Fig. 10. p_t distribution of the experimental K^0_S data (full triangles) together with the results of the IQMD model including a repulsive K^0-nucleus potential of 46 MeV (dashed curves) and without potential (dotted curves) [41].

port approach with and without taking into account a repulsive K^0-nucleus potential. For all rapidity bins, but most evidently at mid-rapidity (shown in Fig. 10), data support calculations with the repulsive potential. Our data suggest a repulsive in-medium K^0 potential of about 40 MeV strength which is slightly higher as compared to results obtained from experiments studying K^0_S production off nuclei [42].

The ability of HADES for the selection of displaced secondary vertices arising from week decays and the high statistics accumulated for the collision system Ar + KCl at 1.76 AGeV allowed to investigate the deep sub-threshold production ($\sqrt{s_{NN}} - \sqrt{s_{\rm thr}} = -640$ MeV) of the double-strange $\Xi^-(1321)$ hyperon [43]. The $\Xi^-(1321)$ was reconstructed in the Λ–π^- invariant mass distribution, shown in Fig. 11, thanks to a high-purity signal of Λ identified in the p–π^- invariant mass distribution. Figure 12 shows the ratio of production rates of $\Xi^-(1321)$ and $\Lambda + \Sigma^0$ as a function of the total CM energy in $N + N$ collisions measured by HADES and other high-energy

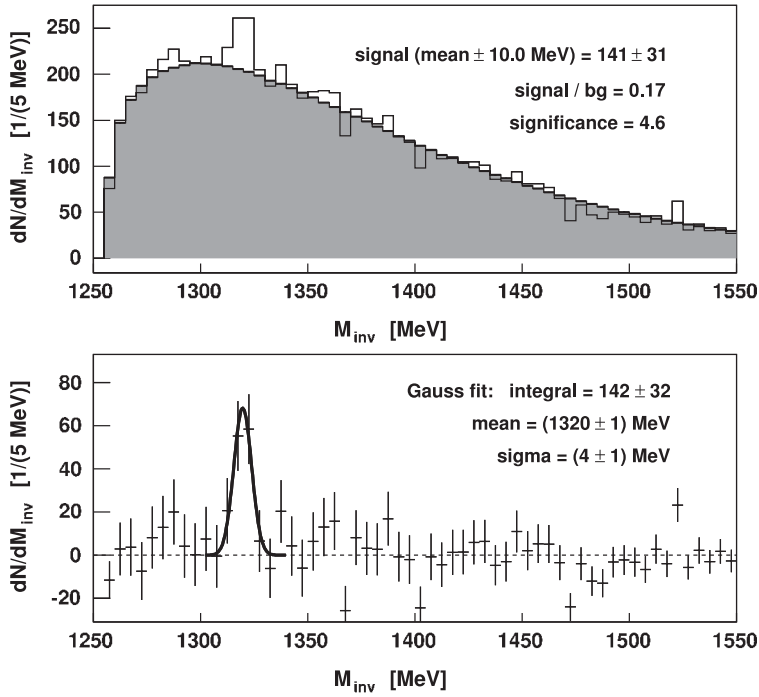

Fig. 11. Top: Λ–π^- invariant mass distribution with background (hatched histogram) calculated with event mixing. Bottom: the invariant-mass distribution after background subtraction. The full curve represents a Gaussian fit to the $\Xi^-(1321)$ signal [43].

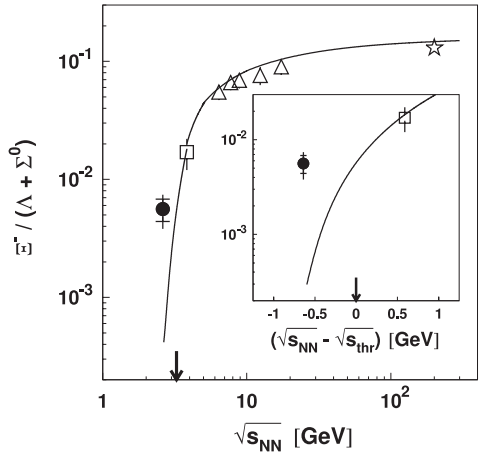

Fig. 12. The excitation function of the $\Xi^-(1321)$ to $\Lambda + \Sigma^0$ ratio measured by HADES (full circles) and other high energy experiments (empty symbols) compared to statistical model predictions [43] (solid curves). The arrow depicts the $\Xi^-(1321)$ threshold [43].

experiments. The reconstructed strength of the signal is compared to calculations performed for Au + Au collisions with the statistical model of [44]. While high-energy data are well described, the present experimental ratio is underestimated, by the model, by a factor of 10 yielding 4×10^{-4}. Utilizing the statistical model package THERMUS [45] and fitting all particle yields, except $\Xi^-(1321)$, measured in Ar + KCl collisions we obtained at temperature $T = 73 \pm 5$ MeV and a chemical potential $\mu_b = 780 \pm$ MeV [46], and the ratio of $\Xi^-(1321)/\Lambda + \Sigma^0$ production even lower (by factor 2) as compared to [44]. In the recent work [47], the strong $\Xi^-(1321)$ production observed in our experiment has been accounted for by strange exchange reactions of the type hyperon–hyperon $\rightarrow N\Xi^-(1321)$. Nevertheless, further high statistics measurements, in particular of the differential production cross sections, are needed to shed more light on this problem.

6. Conclusions

We have presented new results on dielectron and strangeness production in N–N, proton–nucleus and nucleus–nucleus collisions. The e^+e^- invariant mass distributions measured in p+p and p+n collisions at 1.25 GeV reactions provide an important reference for heavy ion collisions. In particular, we find that the anomalous increase of the pair production in $p + n$ collisions, stemming presumably from the bremsstrahlung process, is the main contribution explaining dielectron production in the light C + C collisions. However, we

also observe a significant pair excess in the $0.15 < M_{e^+e^-} < 0.5$ GeV/c^2 mass range with respect to this $N+N$ reference for the medium size Ar + KCl system, indicating an additional contribution from the dense phase of the heavy ion collisions. We interpret this as a result of continuous radiation ("shining") from short lived baryonic resonances (mainly $\Delta(1232)$) regenerated in multi-step processes in dense nuclear matter. An important verification of this scenario will be provided by Au + Au data.

We find that ρ meson production in our energy range is strongly affected by a strong coupling to low-mass baryonic resonances which is reflected in a significant broadening of the meson spectral function already visible in $p+p$ reactions. These interactions might lead to a further meson modification in cold and dense nuclear matter but a quantitative assessment can only be made after these couplings are better constrained.

Studies of the ω production off nucleus show a strong absorption of the meson in nuclear matter in accordance with the results from photon induced reactions. The ω and ϕ signals have also been reconstructed in Ar + KCl collisions at energies below the N–N production threshold. A surprisingly large $R_{\phi/\omega}$ production ratio (more than one order of magnitude larger than in $N+N$ collisions) has been found, indicating no suppression for the ϕ production and consequently a significant contribution to the K^- production. Also a strong enhancement of the double strange $\Xi^-(1321)$ production has been found, even above predictions (factor 10) of statistical models. This intriguing results call for further experimental studies which will be performed with larger collision systems.

Our programme of investigation of the in-medium kaon potential has been started with the measurement of K^0 production in Ar + KCl revealing a strong ($U = 40$ MeV) repulsive potential. Further studies of K_0 potential in cold nuclear matter are on the way with already collected p + Nb data.

The collaboration gratefully acknowledges the support by CNRS/IN2P3 and IPN Orsay (France), LIP Coimbra, Coimbra (Portugal): PTDC/FIS/113339/2009, SIP JU Cracow, Cracow (Poland): 2013/10/M/ST2/00042, Helmholtz-Zentrum Dresden-Rossendorf (HZDR), Dresden (Germany): BMBF 06DR9059D, TU München, Garching (Germany), MLL Munchen DFGEClust: 153VHNG- 330, BMBF 06MT9156 TP5 TP6, GSI TMKrue 1012, NPI AS CR, GSI TMFABI 1012, Rez, Rez (Czech Republic): MSMT LC07050 GAASCRIAA100480803, USC — S. de Compostela, Santiago de Compostela (Spain): CPAN:CSD2007- 00042, Helmholtzalliance HA216/EMMI.

REFERENCES

[1] S. Leupold, V. Metag, U. Mosel, *Int. J. Mod. Phys.* **E19**, 147 (2010).
[2] R. Rapp, J. Wambach, *Adv. Nucl. Phys.* **25**, 1 (2000).
[3] T. Hatsuda, S.H. Lee, *Phys. Rev.* **C46**, 34 (1992).
[4] G.E. Brown, M. Rho, *Phys. Rev. Lett.* **66**, 2720 (1991).
[5] M. Naruki *et al.*, *Phys. Rev. Lett.* **96**, 092301 (2006).
[6] R. Nasseripour *et al.* [CLAS Collaboration], *Phys. Rev. Lett.* **99**, 262302 (2007).
[7] M. Kotulla *et al.* [CBELSA/TAPS Collaboration], *Phys. Rev. Lett.* **100**, 192302 (2008).
[8] M.H. Wood *et al.* [CLAS Collaboration], *Phys. Rev. Lett.* **105**, 112301 (2010).
[9] A. Polyanskiy *et al.* [ANKE Collaboration], *Phys. Lett.* **B695**, 74 (2011).
[10] T. Ishikawa *et al.*, *Phys. Lett.* **B608**, 215 (2005).
[11] G. Agakishiev *et al.* [CERES Collaboration], *Phys. Rev. Lett.* **75**, 1272 (1995).
[12] M. Masera [HELIOS Collaboration], *Nucl. Phys.* **A590**, 93C (1995).
[13] R.J. Porter *et al.* [DLS Collaboration], *Phys. Rev. Lett.* **79**, 1229 (1997).
[14] R. Arnaldi *et al.* [NA60 Collaboration], *Phys. Rev. Lett.* **96**, 162302 (2006).
[15] H. van Hees, R. Rapp, *Nucl. Phys.* **A806**, 339 (2008).
[16] S. Afanasiev *et al.* [Phenix Collaboration], *Phys. Rev.* **C81**, 034911 (2010).
[17] G. Agakishiev *et al.* [HADES Collaboration], *Eur. Phys. J.* **A41**, 243 (2009).
[18] C. Fuchs, *Prog. Part. Nucl. Phys.* **56**, 1 (2006).
[19] G. Agakishiev *et al.* [HADES Collaboration], *Phys. Rev.* **C85**, 054005 (2012).
[20] G. Agakishiev *et al.* [HADES Collaboration], *Phys. Lett.* **B690**, 118 (2010).
[21] J. Weil, H. van Hees, U. Mosel, *Eur. Phys. J.* **A48**, 111 (2012); O. Buss *et al.*, *Phys. Rep.* **512**, 1 (2012).
[22] K. Schmidt *et al.*, *Phys. Rev.* **C79**, 064908 (2009).
[23] M.I. Krivoruchenko *et al.*, *Ann. Phys.* **296**, 299 (2002).
[24] G. Ramalho, M.T. Pena, *Phys. Rev.* **D85**, 113014 (2012).
[25] Q. Wan, F. Iachello, *Int. J. Mod. Phys.* **A20**, 1846 (2005).
[26] W.K. Wilson *et al.* [DLS Collaboration], *Phys. Rev.* **C57**, 1865 (1998).
[27] L.P. Kaptari, B. Kämpfer, *Nucl. Phys.* **A764**, 338 (2006); *Phys. Rev.* **C80**, 064003 (2009).
[28] R. Shyam, U. Mosel, *Phys. Rev.* **C82**, 062201 (2010).
[29] M. Bashkanov, H. Clement, `arXiv:1312.2810 [nucl-ex]`.
[30] G. Agakishiev *et al.* [HADES Collaboration], *Eur. Phys. J.* **A48**, 64 (2012).
[31] G. Agakishiev *et al.* [HADES Collaboration], submitted to *Eur. Phys. J.* **A**.

[32] G. Agakishiev *et al.* [HADES Collaboration], *Phys. Lett.* **B715**, 304 (2012).
[33] M. Nanova *et al.* [CBELSA-TAPS Collaboration], *Phys. Rev.* **C82**, 035209 (2010).
[34] R. Averbeck *et al.* [TAPS Collaboration], *Z. Phys.* **A359**, 65 (1997).
[35] G. Agakichiev *et al.* [HADES Collaboration], *Phys. Lett.* **B663**, 43 (2008).
[36] G. Agakichiev *et al.* [HADES Collaboration], *Phys. Rev.* **C84**, 014902 (2011).
[37] G. Agakishiev *et al.* [HADES Collaboration], *Phys. Rev.* **C80**, 025209 (2009).
[38] H. Schade, Gy. Wolf, B. Kämpfer, *Phys. Rev.* **C81**, 034902 (2010).
[39] R. Arnaldi *et al.* [NA60 Collaboration], *Eur. Phys. J.* **C61**, 711 (2009).
[40] R. Arnaldi *et al.* [NA60 Collaboration], *Eur. Phys. J.* **C64**, 1 (2009).
[41] G. Agakishiev *et al.* [HADES Collaboration], *Phys. Rev.* **C82**, 044907 (2010).
[42] M.L. Benabderrahmane *et al.* [FOPI Collaboration], *Phys. Rev. Lett.* **102**, 182501 (2009).
[43] G. Agakishiev *et al.* [HADES Collaboration], *Phys. Rev. Lett.* **103**, 132301 (2009).
[44] A. Andronic, P. Braun-Munzinger, K. Redlich, *Nucl. Phys.* **A765**, 211 (2006).
[45] S. Wheaton, J. Cleymans, M. Hauer, *Comput. Phys. Commun.* **180**, 84 (2009).
[46] G. Agakishiev *et al.* [HADES Collaboration], *Eur. Phys. J.* **A47**, 21 (2011).
[47] C.M. Ko *et al.*, *Phys. Rev.* **C85**, 064902 (2012).